Available online at www.sciencedirect.com
SCIENCE DIRECT®
Brain Research 997 (2004) 159–164
BRAIN RESEARCH
www.elsevier.com/locate/brainres

Research report

Labeling and dynamic imaging of synaptic vesicle-like microvesicles in PC12 cells using TIRFM

Sheng Xia[a,1], Liang Xu[a,1], Li Bai[a], Zhi-Qing David Xu[a,b], Tao Xu[a,c,*]

[a] *Institute of Biophysics and Biochemistry, Huazhong University of Science and Technology, Wuhan, Hubei, (430074), PR China*
[b] *Department of Neuroscience, Karolinska Institute, S-171 77 Stockholm, Sweden*
[c] *National Key Laboratory of Biomacromoleculars, Institute of Biophysics, Chinese Academy of Sciences, Beijing (100101), PR China*

Accepted 26 October 2003

Abstract

Total internal reflection fluorescence microscopy (TIRFM) was employed to study the trafficking and exocytosis of synaptic vesicle-like microvesicles (SLMVs) in PC12 cells. SLMVs were labeled with vesicular acetylcholine transporter (VAChT) tagged with enhanced green fluorescent protein (EGFP), which displayed punctuate distribution under TIRFM and confocal microscopy. Immunofluorescence analysis confirmed the colocalization of EGFP and VAChT. No significant difference was observed in the distribution or sorting of VAChT when fused either at the N- or the C-terminus. Thus, tagging with GFP does not appear to impair or change the traffic of the VAChT in PC12 cells. Under TIRFM, EGFP-labeled spots moved in a restrained fashion, which resembled that of secretory granules and underwent exocytosis upon stimulation. Together, these data indicate that EGFP-tagged VAChT can be used to explore SLMVs trafficking using TIRFM.

Keywords: Exocytosis; Enhanced green fluorescent protien; Evanescent field; Vesicular acetylcholine transporter; Trafficking

1. Introduction

In the nervous system, neurotransmitters are released from secretory vesicles, which are classified into at least two types of organelles—small synaptic vesicles (SSVs) containing classical neurotransmitters and large dense core vesicles (LDCVs) storing neuropeptides [2,5]. Therefore, vesicle transport and maturation steps preceding membrane merger play an important role in regulating release of transmitter. Though indirect insight was gained by measuring capacitance or optical recording with confocal microscopy, the study of vesicle trafficking has been limited by lack of methods to directly visualize individual vesicles prior to exocytosis in living cells. However, recently, an optical method, so-called total internal reflection fluorescence microscopy (TIRFM), was introduced to study exocytosis [9,15,17,21,22]. In TIRFM, only a thin layer close to the coverslip-solution interface is excited by the so-called evanescent field (EF). Thus, the movement of single vesicles, their docking and fusion as well as the release of dye following exocytosis can be monitored. Direct visualization of fluorescence-labeled LDCVs has been shown by TIRFM in live endocrine [15,17] and epithelial [23] cells. By staining with the fluorescent lipid FM1–43, the docking and fusion of synaptic vesicles have also been captured using TIRFM in goldfish retinal bipolar ribbon synaptic terminals [22]. However, nonspecific FM1–43 staining and its relatively weak fluorescence may limit the observation. In the present study, we labeled synaptic vesicle-like microvesicles (SLMVs), which contain acetylcholine (ACh) in PC12 cells [3] by fusing enhanced green fluorescent protein (EGFP) with vesicular acetylcholine transporter (VAChT), a synaptic

Abbreviations: EF, evanescent field; EGFP, enhanced green fluorescent protein; LDCV, large dense core vesicles; ORF, open reading frame; PCR, polymerase chain reaction; SLMV, synaptic vesicle-like microvesicle; SSV, small synaptic vesicle; TIRFM, total internal reflection fluorescence microscopy; VAChT, vesicular acetylcholine transporter

* Corresponding author. Institute of Biophysics and Biochemistry, Huazhong University of Science and Technology, Wuhan, Hubei, (430074), PR China. Tel.: +86-27-87464577; fax: +86-27-87464577.
E-mail address: txu@mail.hust.edu.cn (T. Xu).
[1] These authors contributed equally to this work.

0006-8993/$ - see front matter © 2003 Elsevier B.V. All rights reserved.
doi:10.1016/j.brainres.2003.10.052

vesicle-specific integral membrane protein. This has allowed analysis of the trafficking and fusion of SLMVs using TIRFM.

2. Materials and methods

2.1. Vectors construction

To construct EGFP-tagged VAChT, the open reading frame (ORF) of VAChT [18] was amplified by polymerase chain reaction (PCR) with *pfu* DNA polymerase (Stratagen, La Jolla, CA) from rat genomic DNA which was isolated from rat tail with DNeasy Tissue Kit (Qiagen, Hilden, Germany). The sequences of VAChT primers are: forward 5′-TATAGAATTCCACCATGGAACCCACCGCGC-CAAC-3′ and reverse 5′-TATAGGATCCCCGCTGCGG-GAGTAATAGTTGTAGTCG-3′. The amplified PCR products were cloned in frame into the *Eco*RI and *Bam*HI sites of the mammalian expression vector pEGFP-N1 and pEGFP-C1 (Clontech Laboratories, Palo Alto, CA).

2.2. Cell culture

The PC12 cells were obtained from the American Type Culture Collection (ATCC, Manassas, VA) and cultured in DMEM (Gibco, Carlsbad, CA) supplemented with 10% horse serum (Gibco) and 5% fetal bovine serum (Gibco). The day prior to the experiment, PC12 cells were transferred onto a poly-L-lysine-coated round coverslip at a density of 50,000 cells per chamber. The external high K^+ solution used to stimulate the PC12 cells was (in mM): 77 NaCl, 60 KCl, 5 $CaCl_2$, 2 $MgCl_2$, 20 glucose, 10 HEPES, pH 7.2. Unless otherwise stated, all drugs were purchased from Sigma.

2.3. Transfection

For transfection, we utilized Effectene Transfection Reagent kit (Qiagen). Two micrograms purified DNA were used for cells cultured in 10-cm^2 flask. Stable cell lines expressing EGFP-tagged VAChT were selected by adding 800 μg/ml of Geneticin (G 418, Invitrogen, Carlsbad, CA) for 21 days. Stably transfected clones were maintained in culture medium containing 200 μg/ml G418 (protocol from Invitrogen website).

2.4. Immunofluorescence

PC12 cells were plated onto poly-L-lysine-coated coverslips in 24-well plate. Cells were fixed with 4% paraformaldehyde and 0.2% picric acide in 0.16 M phosphate buffer solution (pH 7.0) at 4 °C for 20 min and washed by 0.05 M NH_4Cl at 4 °C for 30 min. The cells were incubated overnight at 4 °C with goat polyclonal antiserum to VAChT (1:1000; Chemicon International, Temecula, CA), all in PBS containing 0.3% Triton X-100, 0.02% Bacitracin and 0.1% sodium azide. The cells were then rinsed in PBS for 15–20 min and incubated at 37 °C for 30 min with fluorescein isothiocyanate (FITC)-conjugated donkey anti-goat immunoglobulins (diluted 1:80, Jackson

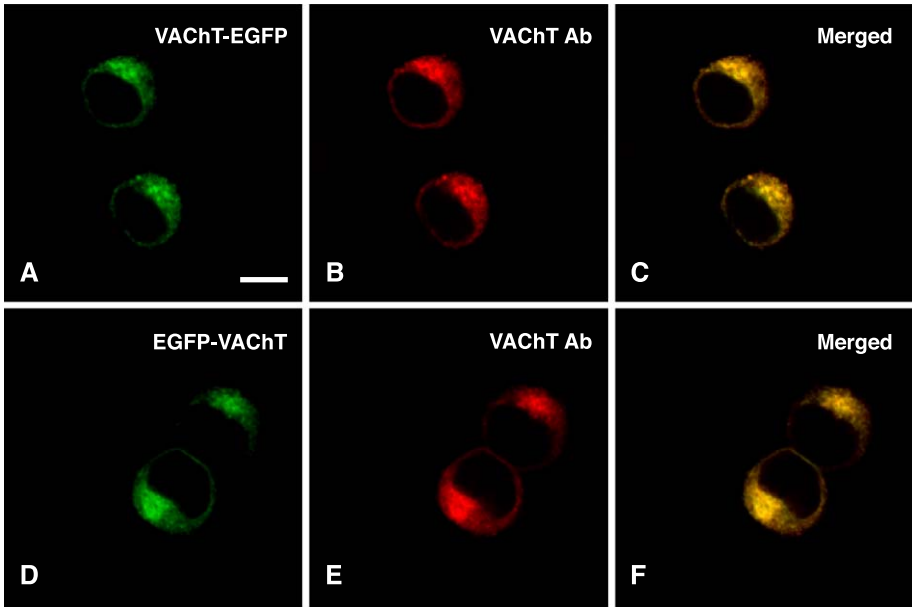

Fig. 1. Intracellular distribution of expressed VAChT-EGFP and EGFP-VAChT. Confocal images of PC12 cells stably expressing VAChT-EGFP (A), EGFP-VAChT (C). PC12 cells transfected with constructs of EGFP-tagged VAChT were immunostained using antibodies against VAChT. The goat polyclonal antiserum to VAChT was detected with a secondary antibody conjugated to RRX (B and D). Double immunofluorescence of the same cells shows that the particulate cytoplasmic localization of EGFP-tagged VAChT coincides with the distribution of VAChT immunoreactivity (C and F). Scale bar is 10 μm.

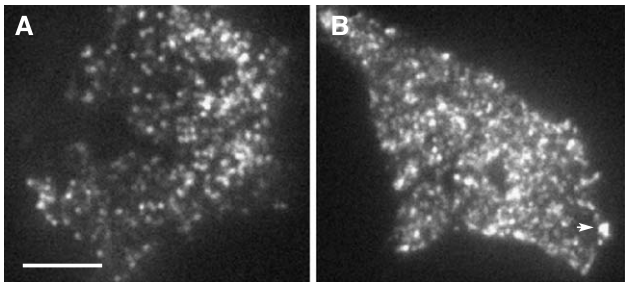

Fig. 2. Distribution of VAChT-EGFP- and EGFP-VAChT-labeled vesicles under TIRFM. TIRFM images of PC12 cells stably expressing VAChT-EGFP (A) and EGFP-VAChT (B). Fluorescence excitation at 488 nm. The arrow indicates a SSLV fusing with the cell membrane. Exposure time is 100 ms. Scale bar is 5 μm.

Immuno Research, West Grove, PA). The cells were rinsed again, mounted in a mixture of glycerol and PBS (3:1) containing 0.1% *para*-phenylenediamine in order to retard fading.

2.5. Confocal imaging

The cells were examined and digital images were acquired using a laser scanning confocal system installed on a Nikon E-600 microscope (Bio-Rad Radiance Plus, Bio-Rad, Hertfordshire, UK). EGFP was exited using a 488-nm argon laser and detected with 530–560-nm band pass filter. Images were collected and processed using Adobe Photoshop (Adobe Systems, San Jose, CA).

2.6. TIRFM imaging collection and analysis

The TIRFM setup was constructed based on the prism-less and through-the-lens configuration as previously described [21]. Briefly, a dual-port condenser (T.I.L.L. Photonics, Gräfelfing, Germany) was used to couple a 488-nm argon ion laser (Melles Griot, Carlsbad, CA) and a Polychrome IV Xenon light source (T.I.L.L. Photonics) to an IX-70 inverted microscope (Olympus, Tokyo, Japan). A micro-prism was placed in the condenser, which can be moved perpendicularly to the optical axis through a micrometer screw in order to adjust the angle at which the laser beam leaves the objective lens. Fluorescence was gathered through a 100× Apo OHR objective (NA 1.65, Olympus) and collected through the left lateral port of the inverted microscope onto an air-cooled SensiCam CCD camera (PCO, Osnabrück, Germany). The interline chip has 1280 × 1024 pixels of 6.7 × 6.7 μm each with "Lens-On-Chip". Images were sampled into the computer through a frame grabber (PCO) with genuine 12 Bit dynamics (4096 gray levels). Piezo Z-drive and E-622 control unit (Physik Instrument, Waldbronn, Germany) were used to control the fine movement of the objective in *Z*-axis.

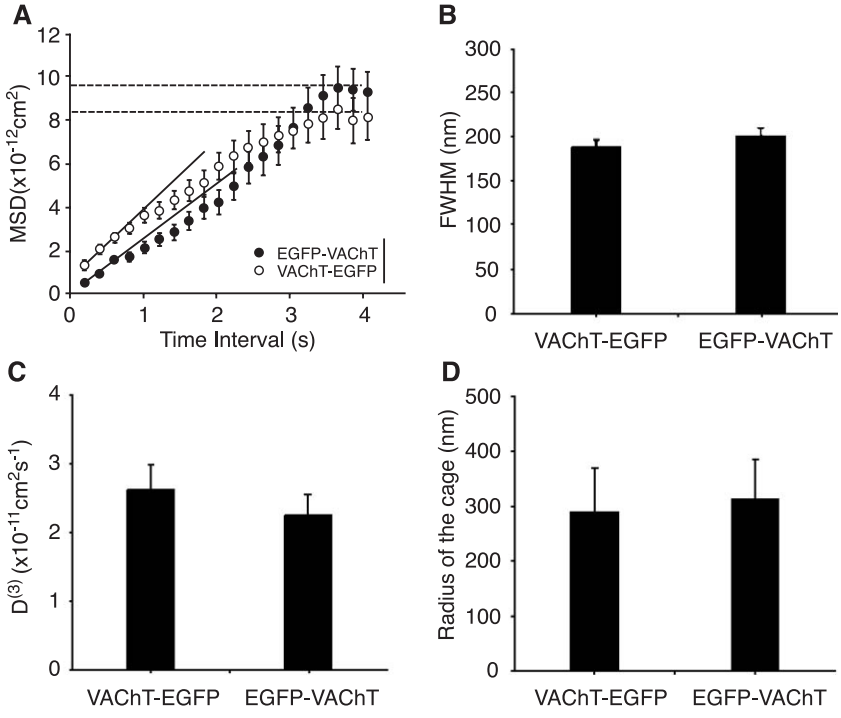

Fig. 3. Comparison of the motion of EGFP-VAChT- and VAChT-EGFP-labeled SLMVs. (A) Plot of the MSD versus observation time Δt for EGFP-VAChT and VAChT-EGFP-labeled SLMVs in PC12 cells. The MSD curve is linear for $\Delta t \rightarrow 0$ while saturating for longer times, consistent with constrained diffusion. (B) Averaged FWHM of VAChT-EGFP and EGFP-VAChT-labeled SLMVs were 189 ± 7 and 201 ± 9 nm. (C) Calculated 3-D diffusion coefficient of vesicle movement, $D^{(3)}$, of the mobile VAChT-EGFP- and EGFP-VAChT-labeled SLMVs. Average $D^{(3)}$ were $2.61 \pm 0.36 \times 10^{-3}$ and $2.25 \pm 0.29 \times 10^{-3}$ $\mu m^2/s$, respectively. (D) Average radius of the cage of VAChT-EGFP- and EGFP-VAChT-labeled SLMVs were 290 ± 80.2 and 315 ± 71.3 nm, respectively.

We used an immersion oil with high refractive index ($n = 1.81$, Cargille Laboratories, Cedar Grove, NJ) to bridge the optical contact between the objective and the coverglass ($n = 1.8$, Olympus). The penetration depth of the evanescent field was determined to be 368 nm as previously described [14,21]. TILL Vision software (V4.0, T.I.L.L. Photonics) was used to control the laser beam and select the wavelength from Polychrome IV for epi-fluorescence illumination. Time-lapsed images were collected with TILL Vision software at frequencies of 2–10 Hz. The exposure time was set from 50 to 500 ms according to the fluorescence intensity of vesicles. Single and time-lapsed images were viewed, processed and analyzed in TILL Vision (T.I.L.L. Photonics) and Adobe Photoshop (Adobe Systems). The dynamics of vesicles were analyzed using Igor Pro (V4.03, WaveMetrics, Lake Oswego, OR) and MatLab (V6.0, The MathWorks, Natick, MA).

3. Results

3.1. Visualization of SLMVs in PC12 cells

PC12 cells were stably transfected with cDNAs encoding VAChT with EGFP attached to the C- or N-terminus (VAChT-EGFP or EGFP-VAChT, respectively). Confocal microscopy analysis of transfected PC12 cells demonstrated that both VAChT-EGFP and EGFP-VAChT were expressed throughout the cytoplasm with a distinct punctuate distribution (Fig. 1A and C). This was similar to that observed for native [6] and expressed [12] VAChT in PC12 cells and distinctly different from the pattern observed in PC12 cells when expressing the EGFP alone (data not shown). No significant fluorescence was observed in the nucleus.

To determine whether the EGFP-tagged VAChT fusion protein is expressed and folded correctly in PC12 cells, we performed immunofluorescence experiments in transfected PC12 cells using antibody against VAChT. Under the confocal microscope, the intense punctuate fluorescence of EGFP coincided with the distribution of VAChT immunoreactivity, as shown in Fig. 1. These results indicate that the chimeras were correctly expressed and labeled SLMVs containing ACh and can be used to track SLMVs in PC12 cells.

We further analysed the EGFP-VAChT- and VAChT-EGFP-transfected PC12 cells under TIRFM, with which illumination of a specimen is restricted to a thin layer of several hundred nanometers. As shown in Fig. 2, there were numerous fluorescent spots in cells transfected with either EGFP-VAChT or VAChT-EGFP. Under resting conditions, the average density of visible spots in transfected PC12 cells was $0.835 \pm 0.387/\mu m^2$ (mean ± S.D., 11 cells), which is much higher than that of LDCVs [11]. The diameter of the fluorescent spots was measured as described in Oheim and Stühmer [8]. The half-maximal width (HFMW) of the VAChT-EGFP- and EGFP-VAChT-labeled SLMVs were 189 ± 7 nm ($n = 18$) and 201 ± 9 nm ($n = 22$), respectively (Fig. 3B).

3.2. Characteristics of the motion of EGFP-VAChT- and VAChT-EGFP-labeled SLMVs

The fluorescent spots were further analysed in time-lapsed recordings under TIRFM to explore motion of VAChT-labeled SLMVs. Stacks of 50 images were processed and analyzed as in Fig. 3A to yield plots of mean square displacement (MSD) against time intervals of 200 ms. The diffusion coefficients were calculated individually from the slope of MSD for the first 3 points [8]. The mean was $2.25 \pm 0.29 \times 10^{-3}$ $\mu m^2/s$ ($n = 10$) for the EGFP-VAChT-labeled SLMVs, which is not significantly different from that of VAChT-EGFP-labeled SLMVs with a mean of $2.61 \pm 0.36 \times 10^{-3}$ $\mu m^2/s$ ($n = 12$) (Fig. 3C). The negative curvatures in the MSD plot as shown in Fig. 3A manifested a constrained diffusion for SLMVs. In constrained diffusion, vesicles motion is assumed to occur in a 'cage' possibly constructed by some cellular structures. The cage radius is equal to the square root of the horizontal asymptote of the MSD plot [8]. The cage of radius restricting the EGFP-VAChT-labeled SLMVs was calculated to be 315 ± 71.3 nm ($n = 10$), while that of the VAChT-EGFP-labeled SLMVs was 290 ± 80.2 nm ($n = 12$) (Fig. 3D).

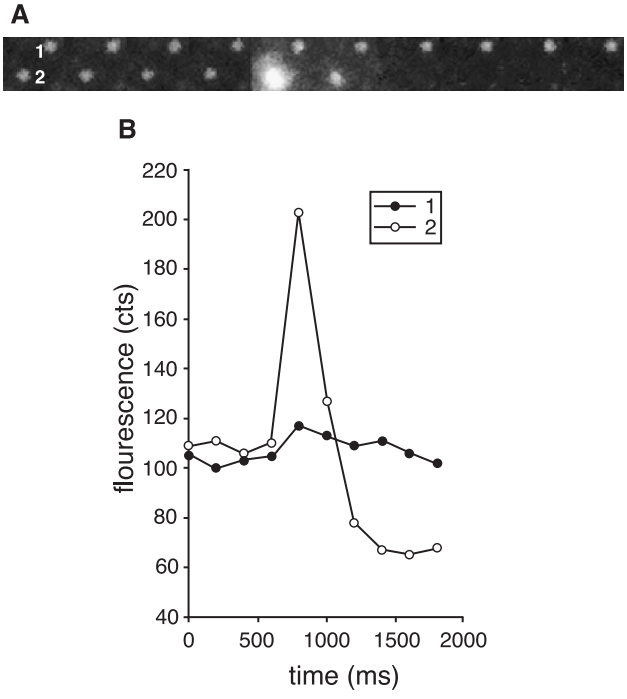

Fig. 4. Time course of the exocytosis of EGFP-VAChT-labeled SLMVs. Time-lapsed images of EGFP-VAChT-transfected PC12 cells were collected at 5 Hz under TIRFM. (A) Sequential images (2×1.8 μm) of single vesicles from the 568–575th image in a stack of 1000. (B) Time course of fluorescence intensity in arbitrary unit of the respective vesicles in (A). High K^+ solution was added at time zero and stopped at 160 s.

3.3. Dynamics of single SLMVs in PC12 cells

To ensure that VAChT-labeled punctuate structures represent functional SLMVs that can undergo exocytosis, we stimulated EGFP-tagged VAChT expressed PC12 cells with external solution containing a high K^+ concentration (60 mM) and imaged for several minutes at 2–10 Hz under EF illumination. Fig. 4A presents the 568–577th image in a stack of 1000. We could observe a green fluorescent spot suddenly brightened followed by a spread of the fluorescence (see also Fig. 4B) as EGFP-tagged VAChT diffused laterally within the plasma membrane after fusion. As a control, a vesicle nearby that did not exocytose showed a constant fluorescence. Similar fusion events were observed for VAChT-EGFP-labeled vesicles (data not shown).

4. Discussion

In the present study, we have analyzed the trafficking dynamics of SLMVs labeled with GFP-tagged VAChT in PC12 cells using TIRFM. One advantage of TIRFM is that only a thin layer close to the glass-solution interface is excitated by the so-called evanescent field. The evanescent field decays exponentially, and its penetration depth (where the intensity declines *e*-fold) is only 30 to a few hundred nanometers. Thus, the influence of out-of-focus background fluorescence is reduced dramatically, which endues TIRFM great spatial sensitivity. Combined with high resolution CCD, TIRFM is very useful in tracking 2-D movement of small particles close to the coverglass. TRIFM is also extremely sensitive to vertical movement. By calibrating the penetration depth and measuring the fluorescence intensities, the vertical movement of objects can be quantitative studied as well. In depth discrimination, TIRFM is up to 10-fold better than confocal microscope. Moreover, TIRFM imaging has a low level of light toxicity and photobleaching. All these advantages make TIRFM a powerful tool to study intracellular organelles underneath the plasma membrane under living conditions [9,14,15,21].

The neuroendocrine cell line PC12 has been used as an in vitro model for studying the biogenesis of synaptic vesicles, since its SLMVs resemble SSVs in size, density, sedimentation and many marker proteins [1]. The VAChT is a vesicle-specific, integral membrane protein that transports ACh into synaptic vesicles [10]. VAChT protein appears predominantly in SSVs/SLMVs [6,11,16,18,20] and has been considered an ideal, specific marker of this type of vesicles in various preparations including PC12 cells [6]. The GFP-tagged version of VAChT has been employed to label SLMVs in PC12 cells [12]. In the present study, we fused EGFP with VAChT at either the N- or C-terminus, and no difference in the subcellular localization of the two chimeras was observed. Both VAChT-EGFP and EGFP-VAChT were recognized as punctuate structures in the cytosol as revealed both by TIRFM and confocal microscopy, similar to that observed for native [6] and expressed [12] VAChT in PC12 cells. Thus, tagging VAChT with GFP does not appear to impair or change the traffic of the protein in PC12 cells. Using immunocytochemistry to localize the GFP chimeras, we confirmed that expressed VAChT tagged with GFP were folded correctly and colocalized with endogenous VAChT. Moreover, EGFP-tagged, VAChT-labeled organelles were found to undergo stimulus-dependent exocytosis, and their motion near the plasma membrane resembled that of secretory granules under TIRFM. Together, these data indicate that EGFP-tagged VAChT can be used to explore SLMVs trafficking using this novel type of microscopy.

Our results demonstrate the existence of large numbers of SLMVs in PC12 cells by using TIRFM. Under evanescent illumination, we found that SLMVs existed in a high density in the sub-plasmalemmal area. This may suggest existence of a large, readily releasable pool (RRP) of SLMVs in PC12 cells. It has been reported based on combined membrane capacitance measurement with amperometry that the fast exocytotic component in PC12 cells mainly comes from the fusion of SLMVs containing ACh [7]. In contrast, the release of catecholamines from LDCVs begins with a delay and proceeds slowly in response to a step-like calcium increase by photolysis of caged-Ca^{2+} in PC12 cells [23]. In contrast, a detailed comparison of amperometric and capacitance signals has demonstrated a sizable RRP of LDCVs in chromaffin cells [4], which leaves little room for the existence of a large pool of SLMVs. Besides the molecular differences in docking and priming mechanisms, the resting $[Ca^{2+}]_i$ level should be considered in view of the Ca^{2+}-dependent priming of the RRP [19,13]. The difference in the state of secretory vesicles and existence of multiple types of vesicles complicate the interpretation of kinetics of exocytosis. Using the present technique, direct visualization of translocation, docking and fusion of different classes of vesicles simultaneously will help to address these problems.

5. Conclusion

The present findings suggest that EGFP-tagged VAChT can be used to explore SLMVs trafficking in PC12 cells. By combining the TIRFM and GFP techniques, individual vesicle trafficking prior to exocytosis has been monitored in living PC12 cells and may allow defining mechanisms underlying the trafficking and fusion of different vesicles.

Acknowledgements

This work was supported by the National Science Foundation of China (Grants 30025023, 3000062 and 30130230), the National Basic Research Program of China (973) (G1999054000 and 2001CCA04100) (to Tao Xu), Harald Jeanssons' Foundation and Harald och Greta

Jeanssons' Foundation (to Zhi-Qing David Xu), the Swedish Medical Research Council (2887), The Marianne and Marcus Wallenberg Foundation and The Knut and Alice Wallenberg Foundation. The laboratory of Tao Xu is also supported by the Partner Group Scheme of the Max Planck Institute for Biophysical Chemistry, Göttingen. We thank Prof. Tomas Hökfelt for making a Bio-Rad confocal microscope available and for advice.

References

[1] L. Clift-O'Grady, A.D. Linstedt, A.W. Lowe, E. Grote, R.B. Kelly, Biogenesis of synaptic vesicle-like structures in a pheochromocytoma cell line PC-12, J. Cell Biol. 110 (1990) 1693–1703.

[2] P. De Camilli, R. Jahn, Pathways to regulated exocytosis in neurons, Annu. Rev. Physiol. 52 (1990) 625–645.

[3] L.A. Greene, G. Rein, Synthesis, storage and release of acetylcholine by a noradrenergic pheochromocytoma cell line, Nature 268 (1977) 349–351.

[4] M. Haller, C. Heinemann, R.H. Chow, R. Heidelberger, E. Neher, Comparison of secretory responses as measured by membrane capacitance and by amperometry, Biophys. J. 74 (1998) 2100–2113.

[5] R.B. Kelly, Storage and release of neurotransmitters, Cell 72 (1993) 43–53(Suppl.).

[6] Y. Liu, R.H. Edwards, Differential localization of vesicular acetylcholine and monoamine transporters in PC12 cells but not CHO cells, J. Cell Biol. 139 (1997) 907–916.

[7] Y. Ninomiya, T. Kishimoto, T. Yamazawa, H. Ikeda, Y. Miyashita, H. Kasai, Kinetic diversity in the fusion of exocytotic vesicles, EMBO J. 16 (1997) 929–934.

[8] M. Oheim, W. Stühmer, Tracking chromaffin granules on their way through the actin cortex, Eur. Biophys. J. 29 (2000) 67–89.

[9] M. Oheim, D. Loerke, W. Stühmer, R.H. Chow, The last few milliseconds in the life of a secretory granule. Docking, dynamics and fusion visualized by total internal reflection fluorescence microscopy (TIRFM), Eur. Biophys. J. 27 (1998) 83–98.

[10] S.M. Parsons, Transport mechanisms in acetylcholine and monoamine storage, FASEB J. 14 (2000) 2423–2434.

[11] M.S. Santos , J. Barbosa Jr., C. Kushmerick, M.V. Gomez, V.F. Prado, M.A.M. Prado, Visualization and trafficking of the vesicular acetylcholine transporter in living cholinergic cells, J. Neurochem. 74 (2000) 2425–2435.

[12] Y. Shoji-Kasai, M. Itakura, M. Kataoka, S. Yamamori, M. Takahashi, Protein kinase C-mediated translocation of secretory vesicles to plasma membrane and enhancement of neurotransmitter release from PC12 cells, Eur. J. Neurosci. 15 (2002) 1390–1394.

[13] C. Smith, T. Moser, T. Xu, E. Neher, Cytosolic Ca^{2+} acts by two separate pathways to modulate the supply of release-competent vesicles in chromaffin cells, Neuron 20 (1998) 1243–1253.

[14] J.A. Steyer, W. Almers, Tracking single secretory granules in live chromaffin cells by evanescent-field fluorescence microscopy, Biophys. J. 76 (1999) 2262–2271.

[15] J.A. Steyer, H. Horstmann, W. Almers, Transport, docking and exocytosis of single secretory granules in live chromaffin cells, Nature 388 (1997) 474–478.

[16] J.H. Tao-Cheng, L.E. Eiden, The vesicular monoamine transporter VMAT2 and vesicular acetylcholine transporter VAChT are sorted to separate vesicle populations in PC12 cells, Adv. Pharmacol. 42 (1998) 250–253.

[17] J.W. Taraska, D. Perrais, M. Ohara-Imaizumi, S. Nagamatsu, W. Almers, Secretory granules are recaptured largely intact after stimulated exocytosis in cultured endocrine cells, Proc. Natl. Acad. Sci. U. S. A. 100 (2003) 2070–2075.

[18] H. Varoqui, J.D. Erickson, The cytoplasmic tail of the vesicular acetylcholine transporter contains a synaptic vesicle targeting signal, J. Biol. Chem. 273 (1998) 9094–9098.

[19] L. von Ruden, E. Neher, A Ca-dependent early step in the release of catecholamines from adrenal chromaffin cells, Science 262 (1993) 1061–1065.

[20] E. Weihe, J.H. Tao-Cheng, M.K. Schafer, J.D. Erickson, L.E. Eiden, Visualization of the vesicular acetylcholine transporter in cholinergic nerve terminals and its targeting to a specific population of small synaptic vesicles, Proc. Natl. Acad. Sci. U. S. A. 93 (1996) 3547–3552.

[21] Z.X. Wu, S. Xia, L. Xu, L. Bai, T. Xu, Dynamic imaging of single secretory granules in live PC12 cells, Acta Biochim. Biophys. Sin. 35 (2003) 381–386.

[22] D. Zenisek, J.A. Steyer, M.E. Feldman, W. Almers, A membrane marker leaves synaptic vesicles in milliseconds after exocytosis in retinal bipolar cells, Neuron 35 (2002) 1085–1097.

[23] D. Zenisek, V. Davila, L. Wan, W. Almers, Imaging calcium entry sites and ribbon structures in two presynaptic cells, J. Neurosci. 23 (2003) 2538–2548.